AIP | Applied Physics Letters

Electric-field-induced phase transformation at a lead-free morphotropic phase boundary: Case study in a 93 % (Bi 0.5 Na 0.5) TiO 3 – 7 % BaTiO 3 piezoelectric ceramic

John E. Daniels, Wook Jo, Jürgen Rödel, and Jacob L. Jones

Citation: Applied Physics Letters **95**, 032904 (2009); doi: 10.1063/1.3182679
View online: http://dx.doi.org/10.1063/1.3182679
View Table of Contents: http://scitation.aip.org/content/aip/journal/apl/95/3?ver=pdfcov
Published by the AIP Publishing

Electric-field-induced phase transformation at a lead-free morphotropic phase boundary: Case study in a 93%$(Bi_{0.5}Na_{0.5})TiO_3$–7% $BaTiO_3$ piezoelectric ceramic

John E. Daniels,[1,a)] Wook Jo,[2] Jürgen Rödel,[2] and Jacob L. Jones[3]
[1]*ID15, European Synchrotron Radiation Facility, Grenoble, Cedex 38043, France*
[2]*Institute of Materials Science, Technische Universität Darmstadt, Darmstadt 64287, Germany*
[3]*Department of Materials Science and Engineering, University of Florida, Gainesville, Florida 32611, USA*

(Received 3 March 2009; accepted 25 June 2009; published online 21 July 2009)

The electric-field-induced strain in 93%$(Bi_{0.5}Na_{0.5})TiO_3$–7%$BaTiO_3$ polycrystalline ceramic is shown to be the result of an electric-field-induced phase transformation from a pseudocubic to tetragonal symmetry. High-energy x-ray diffraction is used to illustrate the microstructural nature of the transformation. A combination of induced unit cell volumetric changes, domain texture, and anisotropic lattice strains are responsible for the observed macroscopic strain. This strain mechanism is not analogous to the high electric-field-induced strains observed in lead-based morphotropic phase boundary systems. Thus, systems which appear cubic under zero field should not be excluded from the search for lead-free piezoelectric compositions. © *2009 American Institute of Physics*. [DOI: 10.1063/1.3182679]

Lead-based piezoelectric ceramics, for example lead zirconate titanate (PZT) or $PbZr_xTi_{1-x}O_3$, display excellent properties at the morphotropic phase boundary (MPB). The MPB in PZT is described as a transformation line where tetragonal and rhombohedral structures coexist.[1] The Landau–Ginsburg–Devonshire phenomenological theory suggests that the Gibbs free energy profile is flattened at the MPB, providing an enhanced response along nonpolar axes.[2] This leads to no or weak preferential polarization orientation.[3] While there is a universal agreement on the presence of enhanced piezoelectric properties in lead-based MPB materials,[4] there has recently been a controversial discussion on the structural nature of the MPB. One view asserts that the MPB region in PZT is of monoclinic structure.[5] A second view describes the monoclinic distortion as observed by x-ray diffraction, as a coexistence of tetragonal and rhombohedral nanodomains.[6,7] Finally, the prototypical MPB in this lead-based piezoelectric material is described not as a sharp border, with all three phases providing a monoclinic distortion.[8] Although the issue is not clearly settled, MPBs are being sought as a starting point for identifying lead-free piezoceramics.[4,9] For example, the solid solution of $(1-x)Bi_{0.5}Na_{0.5}TiO_3-xBaTiO_3$ has been shown to exhibit useful piezoelectric properties at compositions near $x=0.06-0.07$.[10–13] However, subsequent x-ray investigations describe the crystal structure as pseudocubic[14] and transmission electron microscopy investigations have not found a domain structure.[15] Based on electrical measurements, a field-induced phase transformation has been suggested[14,16] and was further corroborated by acoustic emission work.[17] Here, we present electric-field-dependent crystal structure investigations on a BNT-7%BT piezoelectric ceramic in which the structural and microstructural material behavior is monitored by high-energy x-ray diffraction. The results show that the underlying nature of the electric-field-induced strain in these systems is very different from those of lead-containing systems, and is caused by a pseudocubic to tetragonal phase transformation.

High-energy x-ray scattering experiments were carried out at beamline ID15A of the European Synchrotron Radiation Facility. A beam energy of 75.3 keV was selected by a double bent Laue monochromator. Refractive lenses were used to focus the beam to approximately 45×45 μm^2 at the sample. X-ray diffraction images were collected in the forward scattering direction using the Pixium 4700 large area detector.[18] The sample was placed inside an electric-field chamber in which electric fields could be applied perpendicular to the x-ray beam. The use of an area detector allows the measurement of the scattered beam with scattering vector aligned in all directions with respect to the electric-field direction. A more detailed account of this experimental setup can be found elsewhere.[19,20]

The investigated composition BNT-7BT was prepared by conventional solid state processing using stoichiometric fractions of the reagent-grade constituent element oxides and carbonates. Details of the powder preparation can be found elsewhere.[15] A ceramic sample containing a compositional gradient from BNT-7BT to $0.86(Bi_{0.5}Na_{0.5})TiO_3-0.14(K_{0.5}Na_{0.5})NbO_3$ was produced using a method reported previously.[20] The samples were pelletized under a hydrostatic pressure of 300 MPa and sintered at 1150 °C for 3 h embedded in an atmospheric powder to minimize the loss of volatile elements. A sample of dimensions $0.62\times0.72\times3.55$ mm^3 was cut from the sintered ceramic pellet. The respective dimensions are parallel to the directions of the electric field, the x-ray beam, and the orthogonal direction. In the present work, only measurements of the composition BNT-7BT are reported and results of measurements across the compositional grading will be presented elsewhere. In order to confirm this composition, x-ray fluorescence spectra were measured across the sample gradient and into the two end-members. A gradient region in the center of the sample, where atomic diffusion occurred across the boundary, was approximately 0.4 mm wide. The data presented here are measured on a sample position 0.6 mm

a)Electronic mail: jdaniels@esrf.fr.

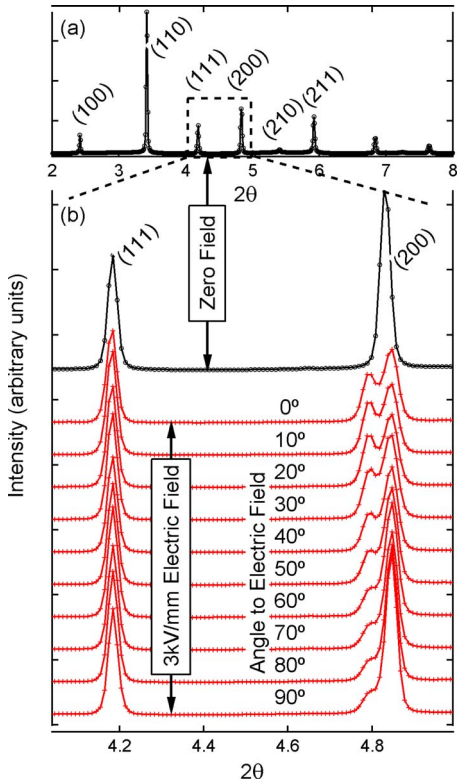

FIG. 1. (Color online) Observed diffraction pattern from BNT-7BT at zero field (a), and selected region (b), both prior to electrical loading (black, top) and under a 3 kV/mm electric field at various angles to the electric field (red, bottom).

from this grading boundary. A ceramic sample of uniform composition (BNT-7BT) was also prepared using the same sintering profile. Silver electrodes were applied to this sample and bulk strain measurements were obtained after electrical poling.

Unipolar strains at fields up to 8 kV/mm were measured on the uniform composition sample at a frequency of 50 mHz. The macroscopically measured electric-field-induced strain at 3 kV/mm was found to be 0.73×10^{-3}, while a strain in excess of 2×10^{-3} was reached at a field strength of 8 kV/mm. Figure 1(a) shows the diffraction pattern from the sample prior to electrical loading. Close inspection of the diffraction pattern shows no profile shape asymmetry or splitting of any reflections, indicating that the sample is cubic or pseudocubic. It has previously been reported that the room temperature structure of this composition is very slightly distorted to either tetragonal or rhombohedral structures,[21] thus the zero-field phase is referred to here as pseudocubic. The region of the diffraction pattern of most interest for the characterization of the electric-field-induced transformation is the (111) and (200) type pseudocubic reflections which are magnified in Fig. 1(b), and presented as a function of the angle between the applied electric field and diffraction scattering vector. Upon application of an electric field of 3 kV/mm, the pseudocubic (200) reflection clearly splits into two peaks, while the pseudocubic (111) reflection remains single and symmetric. This confirms an electric-field-induced structural phase transformation. The single (111) reflection and double (200) reflection is indicative of an electric-field-induced tetragonal phase. From the variation in intensity ratio of the induced (002) and (200) peaks with scattering vector angle to the applied field, it can be concluded that a strong domain texture within the tetragonal phase is present. X-ray measurements of the specimens after electrical loading reveal that the field-induced phase transformation is irreversible. Hence this material should exhibit little fatigue during unipolar cycling, but also does not have the level of unipolar strains as materials with field-induced phase transformation.[14,15]

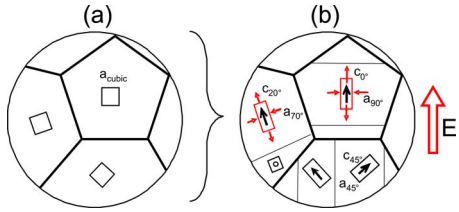

FIG. 2. (Color online) Schematic of domain orientations in response to electric field. In (a), representative grain orientations are shown as a constant pseudocubic lattice parameter prior to electric-field application. In (b), the grain orientations are retained and the electric-field-induced tetragonal domain structure exhibits an orientation dependence of the lattice parameters and domain volume fractions.

A schematic diagram of the electric-field-induced transformation for selected grains is proposed in Fig. 2. Here, it can be seen that the application of an electric field to the sample results in grains of pseudocubic symmetry transforming to tetragonal symmetry. This transformation is accompanied by the grains segregating into ferroelectric domains, with *c*-axis components preferentially aligning as close as possible to the electric field. This indicates that a ferroelectric polarization is formed along this axis. It is interesting to note that at angles perpendicular to the applied electric field, a tetragonal phase is also induced [Fig. 1(b), bottom]. There is no electric driving force for this to take place since the polarization vector of the long *c*-axis is perpendicular to the applied electric field. This behavior may be rationalized by micromechanical strains introduced by the transformation of surrounding grains. That is, within a local neighborhood of grains the majority will be transformed driven by the electric field, these grains elongate parallel to the electric field and contract perpendicular. In order to compensate for this stress on the local microstructure, a minority of grains are mechanically deformed in the opposite sense.

The intensity ratios and positions of the pseudocubic reflections were extracted by multipeak fitting of the raw data using a parametric-type fit[19] of two asymmetric pseudo-Voigt profiles. The fit was constrained such that the peak shapes were consistent throughout all data sets, and also that the intensity ratio varied smoothly and periodically. Figure 3 shows both the extracted lattice parameters and the degree of domain alignment as a function of angle to the electric-field direction. The degree of domain alignment is indicated using f_{002} and calculated as[22]

$$f_{002}(mrd) = 3\frac{\dfrac{I_{(002)}}{I'_{(002)}}}{\dfrac{I_{(002)}}{I'_{(002)}} + 2\dfrac{I_{(200)}}{I'_{(200)}}}, \tag{1}$$

where I' indicates the intensity of the peak in a material with a random distribution of domains. These intensity values are required from an unpoled sample because the scattering power of the (002) and (200) planes may differ. In the case

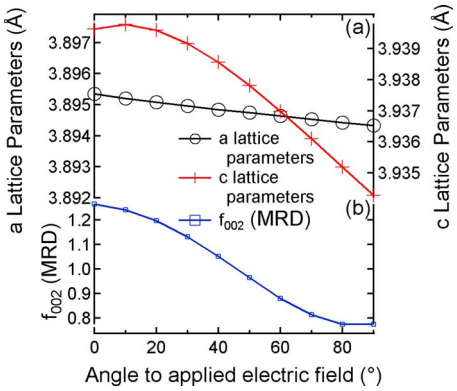

FIG. 3. (Color online) Lattice spacing of the tetragonal phase calculated from the positions of (002) and (200) type peaks (a). Domain texture f_{002} (MRD) calculated from the intensities of (002) and (200) type peaks (b).

of the electric-field-induced transformation, it is not possible to measure the randomly oriented intensities, thus the average intensities of the (002) and (200) peaks over all orientations are used in Eq. (1) for values of $I'_{(002)}$ and $I'_{(200)}$.

The lattice parameters in Fig. 3(a) show that the *c*-axis elongation is maximum parallel to the electric field. This is consistent with the introduction of a polarization vector along the *c*-axis of the unit cell. The figure axes representing the *a* and *c* lattice parameters are scaled to cover an equal magnitude, demonstrating that the *c* lattice parameter is a stronger function of angle than the *a* lattice parameter. The electric-field-induced domain texture shown in Fig. 3(b) exhibits a similar angular dependence to that which occurs in more traditional lead-based MPB materials such as PZT during and after electric-field application.[22,23]

It has been shown that the strain observed in the lead-free piezoelectric material $93\%(Bi_{0.5}Na_{0.5})TiO_3-7\%BaTiO_3$ arises from an electric-field-induced phase transformation from a pseudocubic to a tetragonal structure. The resultant structure under application of an electric field consists of domains, and exhibits a strong domain texture with the spontaneous polarization of the induced phase aligning preferentially parallel to the electric field. The examined sample composition is close to a reported MPB within the BNT-BT system. However, the strain mechanism is clearly different from that of traditional lead-based MPB materials, such as PZT. Good piezoelectric behavior in a system which is pseudocubic under zero electric field also indicates that the search for lead-free alternatives to PZT should not exclude systems which are characterized to be cubic under zero electric field.

[1]B. Jaffe, W. R. Cook, and H. Jaffe, *Piezoelectric Ceramics* (Academic, London, 1971).
[2]D. Damjanovic, J. Am. Ceram. Soc. **88**, 2663 (2005).
[3]G. A. Rossetti, A. G. Khachaturyan, G. Akcay, and Y. Ni, J. Appl. Phys. **103**, 114113 (2008).
[4]T. R. Shrout and S. J. Zhang, J. Electroceram. **19**, 111 (2007).
[5]B. Noheda, D. E. Cox, G. Shirane, J. A. Gonzalo, L. E. Cross, and S.-E. Park, Appl. Phys. Lett. **74**, 2059 (1999).
[6]K. A. Schonau, L. A. Schmitt, M. Knapp, H. Fuess, R.-A. Eichel, H. Kungl, and M. J. Hoffmann, Phys. Rev. B **75**, 184117 (2007).
[7]Y. U. Wang, Phys. Rev. B **76**, 024108 (2007).
[8]A. M. Glazer, P. A. Thomas, K. Z. Baba-Kishi, G. K. H. Pang, and C. W. Tai, Phys. Rev. B **70**, 184123 (2004).
[9]J. Rödel, W. Jo, K. Seifert, E.-M. Anton, T. Granzow, and D. Damjanovic, J. Am. Ceram. Soc. **92**, 1153 (2009).
[10]M. Chen, Q. Xu, B. H. Kim, B. K. Ahn, J. H. Ko, W. J. Kang, and O. J. Nam, J. Eur. Ceram. Soc. **28**, 843 (2008).
[11]B. J. Chu, D. R. Chen, G. R. Li, and Q. R. Yin, J. Eur. Ceram. Soc. **22**, 2115 (2002).
[12]J. Shieh, K. C. Wu, and C. S. Chen, Acta Mater. **55**, 3081 (2007).
[13]T. Takenaka, K. Maruyama, and K. Sakata, Jpn. J. Appl. Phys., Part 1 **30**, 2236 (1991).
[14]S. T. Zhang, A. B. Kounga, E. Aulbach, H. Ehrenberg, and J. Rödel, Appl. Phys. Lett. **91**, 112906 (2007).
[15]S. T. Zhang, A. B. Kounga, E. Aulbach, T. Granzow, W. Jo, H. J. Kleebe, and J. Rödel, J. Appl. Phys. **103**, 8 (2008).
[16]Y. Hiruma, H. Nagata, and T. Takenaka, J. Appl. Phys. **104**, 124106 (2008).
[17]E. Dul'kin, E. Mojaev, M. Roth, W. Jo, and T. Granzow, Scr. Mater. **60**, 251 (2009).
[18]J. E. Daniels and M. Drakopolous, J. Synchrotron Radiat. **16-4**, 463 (2008).
[19]J. E. Daniels, J. Appl. Crystallogr. **41**, 1109 (2008).
[20]J. L. Jones, A. Pramanick, and J. E. Daniels, Appl. Phys. Lett. **93**, 152904 (2008).
[21]R. Ranjan and A. Dviwedi, Solid State Commun. **135**, 394 (2005).
[22]J. L. Jones, E. B. Slamovich, and K. J. Bowman, J. Appl. Phys. **97**, 034113 (2005).
[23]D. A. Hall, A. Steuwer, B. Cherdhirunkorn, P. J. Withers, and T. Mori, Mater. Sci. Eng., A **409**, 206 (2005).